FUNCTION american physiological society

FUNCTION, 2025, 6(3): zqaf020

https://doi.org/10.1093/function/zqaf020
Advance Access Publication Date: 16 May 2025
Original Research

ORIGINAL RESEARCH

Activation of the Carotid Body by Kappa Opioid Receptors Mitigates Fentanyl-Induced Respiratory Depression

Ying-Jie Peng[1], Jayasri Nanduri[1], Ning Wang[1], Zheng Xie[2], Aaron P. Fox[1,2,3], Nanduri R. Prabhakar[1,*]

[1]Institute for Integrative Physiology and Center for Systems Biology of O_2 Sensing, The University of Chicago, Chicago, IL 60637, USA, [2]Department Anesthesia and Critical Care, The University of Chicago, Chicago, IL 60637, USA, [3]Department Pharmacological and Physiological Sciences, The University of Chicago, Chicago, IL 60637, USA

*Address correspondence to N.R.P. (e-mail: nanduri@uchicago.edu)

Abstract

Previous studies reported that opioids depress breathing by inhibiting respiratory neural networks in the brainstem. The effects of opioids on sensory inputs regulating breathing are less studied. This study examined the effects of fentanyl and sufentanil on carotid body neural activity, a crucial sensory regulator of breathing. Both opioids stimulated carotid body afferent nerve activity and increased glomus cell $[Ca^{2+}]_i$ levels. RNA sequencing and immunohistochemistry revealed a high abundance of κ opioid receptors (KORs) in carotid bodies, but no μ or δ opioid receptors. A KOR agonist, like fentanyl, stimulated carotid body afferents, while a KOR antagonist blocked carotid body activation by fentanyl and KOR agonist. In unanesthetized rats, fentanyl initially stimulated breathing, followed by respiratory depression. A KOR agonist stimulated breathing without respiratory inhibition, and this effect was absent in carotid body-denervated rats. Combining fentanyl with a KOR agonist attenuated respiratory depression in rats with intact carotid body but not in carotid body-denervated rats. These findings highlight previously uncharacterized activation of carotid body afferents by fentanyl via KORs as opposed to depression of brainstem respiratory neurons by μ opioid receptors and suggest that KOR agonists might counteract the central depressive effects of opioids on breathing.

Submitted: 5 February 2025; **Revised:** 1 May 2025; **Accepted:** 10 May 2025

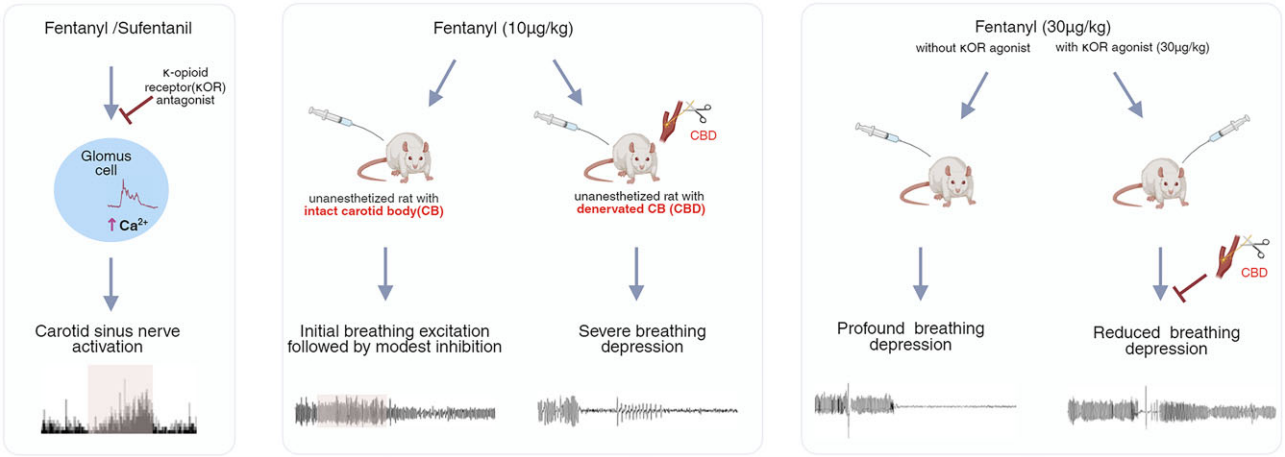

Key words: opioid-induced respiratory depression; arterial chemo receptors; kappa opioid receptors; pre-Bötzinger complex; immunocytochemistry

Introduction

Fentanyl is a widely used opioid in clinics for treating chronic pain and inducing anesthesia. However, the addictive nature of fentanyl often leads to abuse and mortality. A major cause of deaths associated with fentanyl is depression of breathing, known as opioid-induced respiratory depression (OIRD). High prevalence of fentanyl-related deaths prompted investigations on assessing the respiratory responses to fentanyl and other opioids in experimental models and identifying the site(s) and opioid receptors (ORs) mediating breathing depression.

Besides humans, opioids produce respiratory depression in several mammalian species, including cats,[1] rats,[2–5] and mice.[6] Opioid-induced respiratory depression was also reported in frogs,[7] turtles,[8] snakes,[9] and lamprey[10] demonstrating opioids depress breathing in mammalian and non-mammalian species studied thus far.

Brainstem neural networks generate respiratory rhythm. Given that opioids can cross the blood brain barrier, much attention has been focused on investigating the effects of opioids on respiratory rhythm generating neural networks. Three key networks related to breathing have been identified in brainstem, including the pre-Bötzinger Complex (preBötC) generating inspiration, the retrotrapezoid/parafacial nucleus (RTN/pFRG) for activating expiration and CO_2 sensing, and the post-inspiratory complex (PiCo) for post-inspiratory activity.[11] Descending inputs from the Kölliker–Fuse/Parabrachial (KF) nuclei in dorsolateral pons influence these 3 networks. With the exception of RTN/pFRG, opioids inhibit the preBötC, PiCO, and the pontine KF.[12–16]

μ, δ, and k receptors are major ORs identified so far.[17] Targeted genetic deletion of μ-ORs in the preBötC reduces respiratory depression with low but not with high doses of morphine in mice, while deletion of μ-ORs in KF neurons reduces respiratory depression with all doses of morphine.[6] μ-ORs are also implicated in opioid-induced breathing depression in lampreys[10] and snakes.[9] Conversely, δ-ORs are implicated in opioid-induced breathing depression in turtles.[8] These studies suggest that μ-ORs play a major role in opioid-induced inhibition of brainstem respiratory-related neurons, mediating OIRD in mammals.

Breathing is regulated not only by brainstem neural networks but also by chemo- and mechanosensory inputs from the peripheral nervous system (PNS). In 1982, Willette and Sapru[18] reported that systemic application of morphine sulfate caused apnea within a second, along with activation of the recurrent laryngeal nerve, bradycardia, and a biphasic changes in blood pressure (BP) of decerebrate rats. These effects are mediated by the activation of vagal sensory C fibers in the lungs.[18] Similar findings were also recently reported by Zhuang et al.[19] These studies suggest that, unlike brainstem neurons, opioids may activate pulmonary vagal afferents in the PNS.

Carotid bodies are sensory organs for monitoring arterial blood O_2 levels, and carotid body chemoreflex stimulate breathing.[20] Previous studies reported that enkephalins and morphine inhibit carotid body afferent nerve activity.[21,22] However, it is unknown whether fentanyl also inhibits carotid body neural activity. We hypothesized that fentanyl at doses used clinically for minor and major surgeries inhibits carotid body afferent neural activity facilitating respiratory depression. Contrary to our hypothesis, our results showed that fentanyl stimulated carotid body afferent neural activity in rats and elevated $[Ca^{2+}]_i$ in O_2-sensitive glomus cells through kappa opioid receptors (KOR). Furthermore, a KOR agonist stimulated breathing and, and when given with fentanyl reduced respiratory depression, and these effects were absent in carotid body-denervated (CBD) rats.

Materials and Methods

Experimental protocols were approved by the Institutional Animal Care and Use Committee of the University of Chicago (Protocol # ACUP 71810, approved on February 22, 2022). Studies were performed on both male and female adult (age 3-4 months old) Sprague-Dawley rats.

Preparation of Animals for Acute Experiments

Rats were anesthetized with urethane (1.2 g/kg, i.p. Sigma, USA), supplemented hourly with 15% of the initial dose. After tracheal intubation, a femoral artery and vein were cannulated for measuring arterial BP (CWE, Inc., model TA-100) and for intravenous administration of fluids and drugs. Animals were paralyzed with

pancuronium bromide (2.5 mg/kg/h, iv, Sigma, #P1918) to prevent spontaneous breathing. Rats were mechanically ventilated (Kent Scientific, model RoVent) with oxygen-enriched room air. Rectal temperature was maintained at 38 ± 1°C using a heating pad. At the end of the experiments, animals were euthanized with an intravenous administration of euthanasia.

In Vivo Measurements of Carotid Body Sensory Activity

Carotid body sensory nerve activity was recorded in anesthetized rats as previously described.[23] The carotid bifurcation was isolated, and the carotid sinus nerve was transected at its junction with the glossopharyngeal nerve. Sensory nerve activity was recorded using a monopolar platinum-iridium wire electrode, with a reference electrode placed in a nearby neck muscle. Electrical activity was amplified by an AC amplifier (Grass, P511K) with a bandwidth of 100–3000 Hz and displayed on an oscilloscope (Tektronix, TDS2012). Action potentials above baseline noise were converted to standardized pulses using a window discriminator (WPI, model 121). The output was fed into a rate meter (CWE, RIC-830) to display integrated neural activity. Signals from the rate meter, raw action potentials, and BP were continuously recorded and stored via a data acquisition system (Power Lab/8P, AD Instruments) for further analysis. Carotid body sensory activity was identified by increased nerve activity in response to hypoxia and decreased activity by hyperoxia (100% O_2). Occluding the common carotid artery for 10 s caused no change or an increase in sinus nerve activity, indicating the sensory activity originated from the carotid body rather than carotid baroreceptors. Fentanyl dissolved in saline (0.3 mL, Sigma, #F-013) was administered through the femoral vein catheter over a 1 min period.

Ex Vivo Measurements of Carotid Body Sensory Activity

Sensory nerve activity from *ex vivo* carotid body was recorded as previously described.[24,25] Briefly, carotid bodies along with the sinus nerves were harvested from urethane anesthetized rats, placed in a recording chamber (volume, 250 μL), and superfused with warm physiological saline (35°C) at a rate of 3 mL/min. The composition of the medium was (mM): NaCl, 125; KCl, 5; $CaCl_2$, 1.8; $MgSO_4$, 2; NaH_2PO_4, 1.2; $NaHCO_3$, 25; D-Glucose, 10; Sucrose, 5. The solution was bubbled with 21% O_2/5% CO_2 balanced room air, and hypoxic challenges were achieved by switching the perfusate to physiological saline equilibrated with 5% O_2/5% CO_2 balanced room air. Carotid body sensory nerve responses to fentanyl and/or OR agonists/antagonists were examined by switching the perfusate to physiological saline containing corresponding compounds for 5 min. To facilitate recording of clearly identifiable action potentials, the sinus nerve was treated with 0.1% collagenase for 5 min. Action potentials (1–3 active units) were recorded from one of the nerve bundles with a suction electrode (band pass 30 Hz–10 kHz) and stored in a computer via a data acquisition system (PowerLab/8P), and the sampling rate was set at 10 kHz. "Single" units were sorted based on the shape, height, and duration of the individual action potentials using the spike discrimination module.

Primary Cultures of Glomus Cells

Protocols for preparing primary glomus cell cultures are the same as previously described methods.[26] Briefly, carotid bodies were harvested from urethane-anesthetized rats, and glomus cells were dissociated using collagenase P (2 mg/mL), DNase I (15 μg/mL), and BSA (3 mg/mL) at 37°C for 20 min, followed by a 15-min incubation in Locke's buffer with DNase I (30 μg/mL). Cells were plated on collagen-coated coverslips and maintained at 37°C in a 7% CO_2 + 20% O_2 incubator for 12–18 h. The growth medium consisted of DMEM/F-12 medium, supplemented with 1% fetal bovine serum, insulin-transferrin-selenium (ITS-X), and 1% penicillin-streptomycin-glutamine mixture.

Measurements of $[Ca^{2+}]_i$

$[Ca^{2+}]_i$ in glomus cells was measured as described previously.[26] Briefly, glomus cells on a coverslip were incubated in Hanks' balanced salt solution with 2 μM fura-2 AM and 1 mg/mL BSA for 30 min, then washed in a fura-2-free solution for another 30 min at 37°C. The coverslip was transferred to a chamber for measuring intracellular calcium concentration $[Ca^{2+}]_i$. Background fluorescence was collected at 340- and 380-nm wavelengths from an area devoid of cells. Glomus cells were identified by their characteristic clustering, and individual cells were imaged using a Leica microscope with a Hamamatsu camera and HC Image software. Image pairs (340 nm and 380 nm) were obtained every 2 s by averaging 16 frames at each wavelength. Data were continuously collected throughout the experiment, and background fluorescence was subtracted from the cell data at each wavelength. Fluorescence intensity was calculated by dividing the 340 nm image by the 380 nm image to obtain a ratiometric image. Ratios were converted to free $[Ca^{2+}]_i$ using calibration curves constructed *in vitro* with fura-2 (50 μM free acid) in solutions containing known Ca^{2+} concentrations (0–2000 nM). The recording chamber was continually irrigated with warm physiological saline (31°C) from gravity-fed reservoirs, with the same composition as that used for recording carotid body sensory nerve activity.

RNA Sequencing of ORs

RNA sequencing was performed as previously described.[27] Carotid bodies were collected from anesthetized rats. Total RNA was isolated (n = 8 carotid bodies/experiment, n = 3 experiments) using Direct-zol RNA Microprep Kits (Zymo Research, R2060, Irvine, CA, USA) and submitted to the University of Chicago Genomics Core Facility (RRID: SCR_019196) for sequencing. cDNA library construction was carried out with 100 ng of total RNA input followed by 100 bp paired-end sequencing (using PolyA + selection) on an Illumina NovaSEQ 6000 platform. The sequencing data were processed by the University of Chicago's CRI Bioinformatics Core. The quality of raw sequencing reads was assessed with FastQC. Uniquely mapped reads of *Oprμ1*, *Oprδ1*, and *Oprκ1* were obtained by aligning the FASTQ files to the rat reference transcriptome (Rnor_6.0.102) using STAR version 2.6.1d. Relative gene expression levels were summarized and expressed as Fragments Per Kilobase of transcript per million mapped reads (FPKM). The raw RNA-seq data are accessible via GEO (GSE #252955).

Immunohistochemistry of ORs

Immunohistochemistry of the carotid body and brainstem was performed as described previously.[28,26] Briefly, anesthetized rats (urethane 1.2 g/kg, ip) were perfused transcardially with heparinized PBS (pH 7.4) at a rate of 30 mL/min for 10 min, followed by PBS-buffered 4% paraformaldehyde (Sigma, #158127) for 30

min. Carotid bifurcations and brainstems were removed, post-fixed in 4% paraformaldehyde for 3 and 24 h, respectively, and cryoprotected in 30% sucrose–PBS at 4°C for 24 h. Frozen tissues were serially sectioned at a thickness of 8 μm (carotid bodies) or 30 μm (brainstems, coronal section) and stored at –80°C. Sections were treated with PBS containing 10% normal goat serum and 0.2% Triton X-100 for 30 min and then incubated with primary antibodies in PBS containing 1% normal goat serum and 0.05% Triton X-100 at 4°C for 24 h, followed by 3 washes with PBS containing 0.05% Triton X-100. Sections were then incubated with a secondary antibody at room temperature for 1 h, followed by 5 washes with PBS containing 0.05% Triton X-100. Sections were mounted in Vectashield with DAPI (Vector Laboratories, #H-1200) and visualized using an all-in-one fluorescent microscope (BZ-X810; Keyence Corp. of America, Itasca, IL). The anatomical location of the preBötC was identified based on an adult brain atlas.[29]

Carotid body sections were treated with a primary antibody against tyrosine hydroxylase (TH) and another against an anti-opioid receptor antibody (MOR-1, DOR-1, or KOR-1), while brainstem sections were treated with an anti-Neurokinin-1 receptor (NK1R) antibody and another against an anti-opioid receptor antibody (MOR-1 or KOR-1). The primary antibodies used were rabbit anti-TH antibody (Pel-Freez Biologicals; #P40101-0; dilution 1:1000), mouse anti-TH antibody (Sigma, #T1299, dilution 1:1000), guinea pig anti-NK1R antibody (Millipore, AB15810, dilution 1:500), rabbit anti-NK1R antibody (Novus Biologicals, NB300-119B, dilution 1:250), mouse anti-KOR-1 antibody (Santa Cruz, sc-374479; dilution 1:200), mouse anti-MOR-1 antibody (Santa Cruz, sc-515933; dilution 1:200, for carotid bodies), rabbit anti-MOR-1 antibody (Sigma, ZRB2031, dilution 1:500, for brainstems), and rabbit anti-DOR-1 antibody (Abcam, ab176324; dilution 1:200). The secondary antibody (dilution 1:250) used for detecting binding of TH or NK1R was either Alexa Fluor 488-conjugated goat anti-mouse IgG (Thermo Fisher Scientific, A11029) or goat anti-rabbit IgG (Thermo Fisher Scientific, A11034), and for detecting binding of ORs was Alexa Fluor 555-conjugated goat anti-mouse IgG (Thermo Fisher Scientific, A21424), goat anti-guinea pig IgG (Thermo Fisher Scientific, A21435), or goat anti-rabbit IgG (Thermo Fisher Scientific, A21429).

Jugular Vein Catheter and Temperature Microchip Implantation

Rats were anesthetized with isoflurane (4% induction, 1.5% maintenance). A polyurethane venous catheter (Instech Laboratories) filled with 0.9% saline was implanted into the right external jugular vein under aseptic conditions for administering fentanyl and/or KOR agonist. The catheter was tunneled subcutaneously and exteriorized at the nape of the neck. A temperature microchip (UCT-2112, Unified Information Devices) was injected subcutaneously into the midback, and body temperature was monitored using an RFID reader (URH-300HP, Unified Information Devices) during experiments.

Carotid Body Denervation

The carotid artery bifurcation area was exposed through a midline incision of approximately 1 cm at the anterior neck in rats under isoflurane anesthesia. The carotid sinus nerve was identified where it joins the glossopharyngeal nerve and was cut. Sham-operated rats served as controls.

Breathing Measurements in Conscious Rats

Rats with jugular vein implant, sham, and CBD rats were allowed from surgical recovery for 7 days. Breathing was monitored in these rats without anesthesia with whole body plethysmography (Buxco, DSI, St. Paul, MN) as described previously.[30,31] Respiratory variables (breathing rate, tidal volume, and minute ventilation) and duration of apnea were measured. Sighs, sniffs, and movement-induced changes in breathing variables were excluded from the analysis. Rats were acclimated to the plethysmograph chamber for 1 h. All measurements were made between 9:00 AM and 12:00 PM at ambient temperature (~25°C) to exclude influence from circadian variation. Three groups of experiments were performed: *Group 1*: Breathing response to fentanyl in sham and CBD rats ($n = 7$ each). Baseline breathing was monitored for 5 min, and then 0.3 mL of vehicle (saline) was administered through the jugular venous catheter over 1 min, and breathing was monitored continuously for 30 min. The protocol was repeated with fentanyl (10 μg/kg in 0.3 mL saline, Sigma, #F-013). *Group 2*: Breathing response to κ-OR agonist (U-50488, Tocris Biosciences, #0495) in sham and CBD rats ($n = 6$ each). *Group 3*: Effect of κ-OR agonist (U-50488) on fentanyl-induced breathing depression ($n = 6$ rats). Day 1—breathing response to fentanyl alone, Day 2—breathing response to combined administration of κ-OR agonist with fentanyl was monitored for 45 min.

Analysis of the Data and Statistical Measures

Carotid body sensory activity (single units) was averaged for 2 min prior to and during the entire period of compound application and expressed as impulses per second (Hz) unless otherwise stated. At least 2-3 single units were analyzed in each carotid body in a given experiment. All data were normalized to baseline and presented as individual data points along with mean ± SEM and were plotted using GraphPad Prism (version 8). Statistical analysis began with testing assumptions of normal distribution (Shapiro–Wilk test) and equal variances (Levene's median test). If both assumptions were satisfied, a paired *t*-test or *t*-test was performed. Otherwise, the Wilcoxon signed-rank test or Mann–Whitney rank sum test was applied. The effect of different doses of fentanyl on carotid body sensory activity *ex vivo* was analyzed using one-way repeated measures ANOVA on ranks followed by Dunn's test. The excitatory effect of fentanyl on breathing was analyzed using 2-way ANOVA with repeated measures followed by the Holm–Sidak test. All statistical analyses were performed using SigmaPlot (version 11), and *P*-values $< .05$ were considered significant.

Results

Fentanyl Stimulates Carotid Body Afferent Nerve Activity

The effect of intravenous fentanyl on carotid body sensory nerve activity was examined in urethane-anesthetized, mechanically ventilated rats. Arterial BP and carotid body afferent nerve activity were recorded. Two doses of fentanyl (10 and 100 μg/kg) equivalent to human doses of 1.6 and 16.1 μg/kg, respectively, were tested. A dosage of 2 μg/kg is recommended for minor surgery, while 2–20 μg/kg is recommended for major surgery.[32]

Examples illustrating the carotid body sensory nerve and BP responses to 2 doses of fentanyl are shown in Figure 1A. Both doses stimulated the carotid body activity (Figure 1A and B;

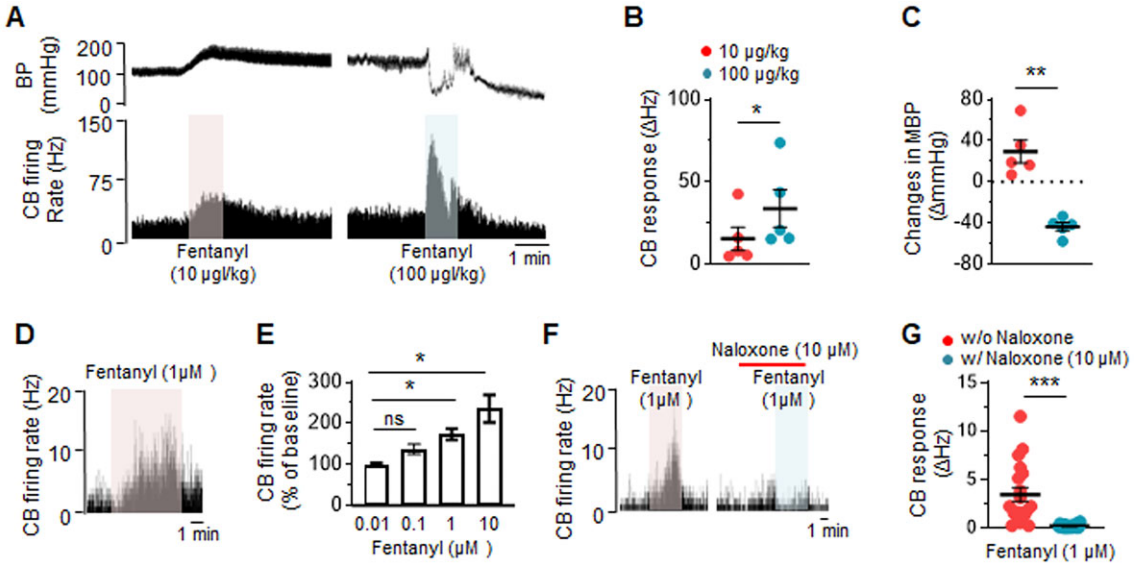

Figure 1. Fentanyl stimulates carotid body (CB) afferent neural activity. (A) Examples of *in vivo* carotid body afferent and blood pressure (BP) responses to 2 doses of fentanyl in anesthetized rats. (B-C) Individual and mean ± SEM of carotid body afferent nerve activity (presented as fentanyl-vehicle baseline carotid body afferent firing rate, Δ Hz, B) and mean BP (MBP, fentanyl-baseline BP, Δ mmHg, C) responses to fentanyl from 5 rats. (D) Examples of *ex vivo* carotid body afferent nerve response to fentanyl. (E) Mean ± SEM of dose-response of *ex vivo* carotid body afferent nerve firing rate (% of vehicle baseline) to fentanyl from 10 carotid bodies from 5 rats. (F) Examples of carotid body afferent nerve activation by fentanyl in the absence or presence of naloxone. (G) Mean ± SEM and individual data of responses to fentanyl in the absence or presence of naloxone from 19 afferents from 7 carotid bodies. Shaded areas in (A), (D), and (F) and horizontal bar in F indicate the duration of drug application. ∗, and ns denotes $P < .05$ and $P > .05$, respectively, in (E), one-way repeated measures ANOVA on ranks followed by the Dunn's test. ∗, ∗∗, and ∗∗∗ denote $P < .05$, .01, and .001, respectively, in (B), (C), and (G), paired *t*-test.

$P < .05$). While low dose of fentanyl (10 μg/kg) increased BP, high dose (100 μg/kg) decreased BP (Figure 1A and C; $P < .001$ compared to low dose). A decrease in BP by itself can stimulate the carotid body.[20] To avoid confounding influence of BP, carotid body activity was examined in an *ex vivo* superfused carotid body preparation. The effects of 0.01–10 μM fentanyl were tested on *ex vivo* carotid bodies. The concentration of 1 μM fentanyl in rats is equivalent to a human dose of 3.8 μg/kg (assuming a blood volume of about 21 mL in 300 g rat). Fentanyl increased *ex vivo* carotid body sensory nerve activity in a dose-dependent manner (Figure 1D and E).

To assess whether carotid body activation by fentanyl involves ORs, the response to 1 μM fentanyl was determined in the absence or presence of 10 μM naloxone, a pan-OR antagonist. Naloxone blocked carotid body activation by fentanyl (Figure 1F and G), indicating participation of ORs.

Opioid Receptors in the Carotid Body

Naloxone primarily targets μ-ORs but can also affect δ and κ receptors.[17] Given the limited information of ORs in the rat carotid body, RNA sequencing was used to analyze genes encoding ORs. κ-OR mRNA was abundant, while μ- and δ- OR mRNAs were undetectable (Figure 2A). Immunocytochemistry confirmed these findings: μ- and δ- OR-like immunoreactivities were not detected, whereas many glomus cells were positive for κ-ORs, indicated by co-localization with TH, a marker of these cells (Figure 2B).[20,33]

Validation of Antibodies

Antibodies were validated not only by omitting the primary antibody but also with immunohistochemistry of OR expression in brainstem neurons of the same rats used for carotid body immunocytochemistry. k- and μ-OR-like immunoreactivity was assessed in the preBötC. PreBötC neurons were identified with neurokinin-1 (NK-1)-like immunoreactivity, a marker of preBötC neurons (Figure 2C).[34,35] k-OR-like immunoreactivity was not detected in the preBötC, whereas μ-OR-like immunoreactivity was observed in nerve fibers adjacent to preBötC neurons (Figure 2C).[34,35] However, k-OR-like immunoreactivity was detected in neurons of the nucleus raphe obscurus, another brainstem area (Figure S1).

The roles of μ- and k-ORs were further assessed by monitoring carotid body afferent nerve responses to DAMGO ([D-Ala2, N-MePhe4, Gly-ol]-enkephalin), a highly selective μ-OR agonist, and U-50488H, a selective k-OR agonist. While 10 μM DAMGO had no effect, 1 μM U-50488H stimulated carotid afferent nerve activity (Figure 2D-E), indicating low abundance of μ-OR and a high abundance of k-OR in the carotid body.

KOR Antagonist Blocks Carotid Body Activation by Fentanyl

We studied the effect of the KOR antagonist aticaprant on carotid body afferent nerve responses to fentanyl and a KOR agonist U-50488H. Aticaprant at 100 nM effectively blocked carotid body activation by both fentanyl and U-50488H (1 μM each) ($P < .001$; Figure 3A–D).

Sufentanil, A Fentanyl Analogue Activates Carotid Body

Sufentanil, a fentanyl derivative, is another widely used opioid analgesic. To determine if carotid body activation is selective to fentanyl, carotid body afferent nerve responses to sufentanil were analyzed. While vehicle has no effect (Figure 4A; *left panel*), sufentanil at 50 and 100 nM stimulated carotid body neural activity (Figure 4A and B). The activation magnitude with 100 nM sufentanil was comparable to 1 μM fentanyl (100 nM

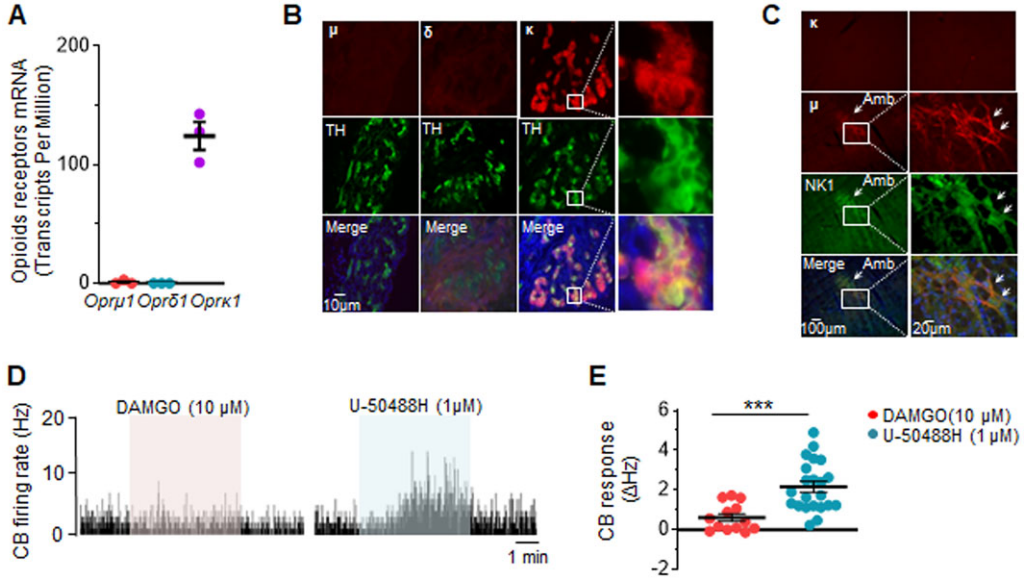

Figure 2. Opioid receptors in the rat carotid body. (A) mRNA abundance of *Oprμ*, *δ*, and *k*. Shown are mean ± SEM and individual data from 3 experiments ($n = 8$ carotid bodies/experiment, from 12 rats). (B) Immunohistochemistry of μ, *δ*, and *k* in carotid body sections. Tyrosine hydroxylase (TH) immunoreactivity was determined as a marker of glomus cells. Magnified images of square boxes in the right panel. (C) k and μ like immunoreactivities in the preBötC neurons identified by neurokinin-1 like immunoreactivity. (D) Examples of carotid body afferent nerve responses (carotid body firing rate, Hz) to DMAGO and U-50488H, a k-opioid receptor agonist. (E) Carotid body afferent nerve response presented as mean ± SEM and individual data from $n = 13$ and 22 individual carotid body afferents from 6 and 8 carotid bodies, respectively. Shaded areas in (D) indicate duration of drug application. *** denotes $P < .001$, *t*-test.

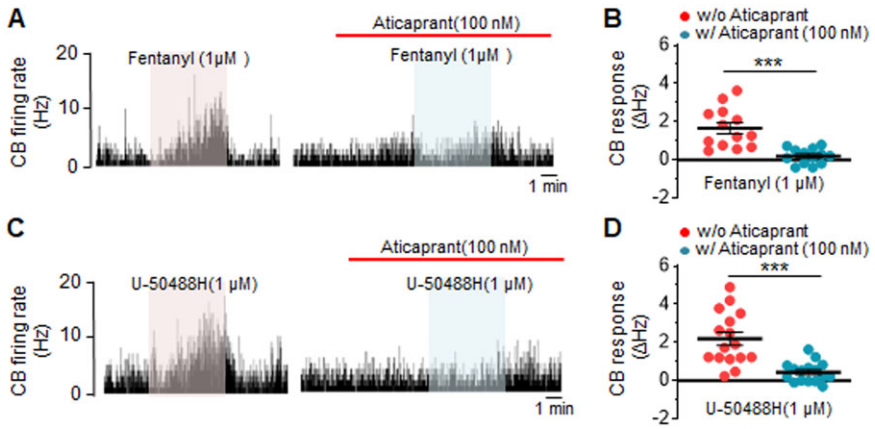

Figure 3. A KOR antagonist blocks fentanyl- and KOR agonist-evoked carotid body afferent nerve activation. (A) Examples of carotid body afferent nerve activation by fentanyl in the absence or presence of aticaprant (a KOR antagonist). (B) Mean ± SEM and individual data of responses to fentanyl in the absence or presence of aticaprant from 13 afferent fibers from 6 carotid bodies. (C) Examples of carotid body afferent nerve activation by a KOR agonist (U-50488H) in the absence or presence of aticaprant. (D) Mean ± SEM and individual data of responses to U-50488H in the absence or presence of aticaprant from 16 afferents from 7 carotid bodies. Data in (B) and (D) represents drug-vehicle baseline afferent nerve activity (carotid body response, ΔHz). Shaded areas and horizontal bars in (A) and (C) indicate the duration of drug application. *** indicates $P < .001$, paired *t*-test.

sufentanil = +98.7 ± 7.7% vs 1 μM fentanyl = +93.2 ± 10.5%; $P = .173$) indicating greater potency of sufentanil than fentanyl. Additionally, 100 nM aticaprant, a KOR antagonist, blocked carotid body nerve activation by sufentanil (Figure 4C and D).

Glomus Cell Responses to Fentanyl and Sufentanil

Carotid body afferent nerve activation requires $[Ca^{2+}]_i$ elevation in glomus cells. Therefore, glomus $[Ca^{2+}]_i$ responses to fentanyl and sufentanil were determined. Both fentanyl (1 μM) and sufentanil (100 nM) elevated $[Ca^{2+}]_i$ in glomus cells, and this response was completely blocked by the aticaprant (100 nM), a KOR antagonist (Figure 5A–D).

Breathing Responses to Fentanyl and KOR Agonist

Carotid body afferent activation stimulates breathing.[20] We explored whether carotid body activation by fentanyl and KOR agonist stimulate breathing. Breathing was monitored in unanesthetized rats with intact carotid bodies and in rats that underwent carotid body denervation (CBD) 7 days prior. Sham-operated rats served as controls. Catheters were implanted in the jugular vein under isoflurane anesthesia for administering either fentanyl or a KOR agonist.

Breathing responses to 10 μgm/kg fentanyl (human equivalent dose for minor surgery) were assessed in both sham-operated and CBD rats, as this dose activated carotid body in anesthetized rats (see Figure 1A).

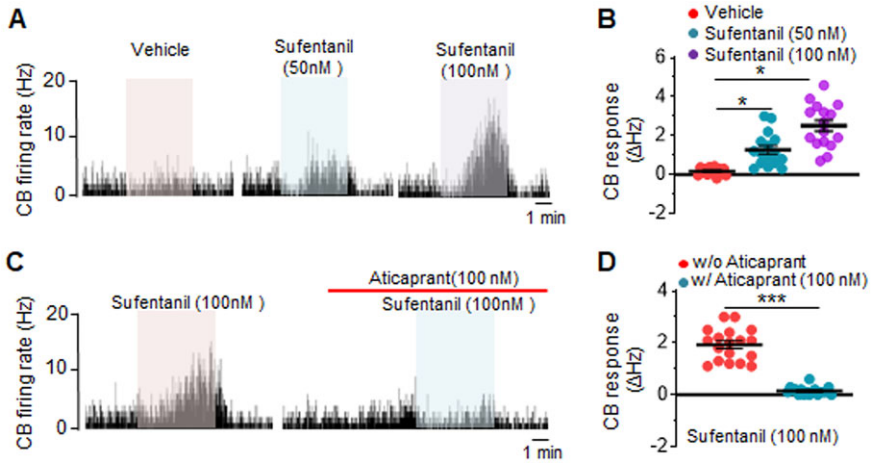

Figure 4. Sufentanil, a fentanyl analogue, stimulates carotid body afferent nerve activity. (A) Examples of *ex vivo* carotid body responses to vehicle (0.02% methanol) and 2 concentrations of sufentanil. (B) Mean ± SEM and individual data of carotid body afferent nerve activation by vehicle (13 afferent fibers from 6 carotid bodies) and 2 concentrations of sufentanil in 15 afferents from 6 carotid bodies. (C) Examples of carotid body afferent nerve activation by sufentanil in the absence or presence of aticaprant. (D) Mean ± SEM and individual data of responses to sufentanil in the absence or presence of aticaprant in 16 afferents from 7 carotid bodies. Data in (B) and (D) represent drug-vehicle baseline afferent nerve activity (carotid body response, ΔHz). Shaded areas in (A) and (C) and horizontal bar in (C) indicate the duration of drug application. (B) ∗ indicates $P < .05$ one-way ANOVA on ranks followed by Dunn's test and D ∗∗∗ indicates $P < .001$, paired *t*-test.

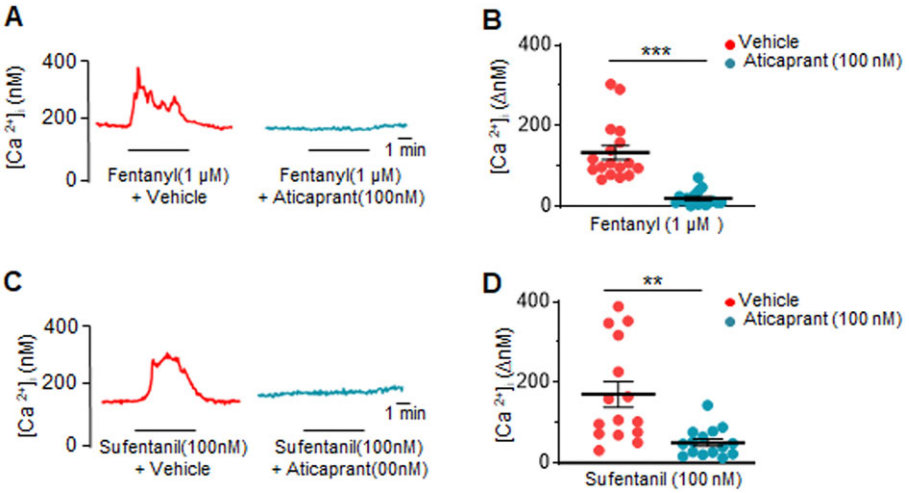

Figure 5. Glomus cell Ca^{2+} response to fentanyl and sufentanil. (A) Examples of glomus cell Ca^{2+} response to fentanyl in the presence of vehicle or aticaprant. (B) Mean ± SEM and individual data of Ca^{2+} response to fentanyl in the presence of vehicle or aticaprant in 17 cells from 12 carotid bodies. (C) Examples of glomus cell $[Ca^{2+}]_i$ response to sufentanil with vehicle or aticaprant. (D) Mean ± SEM and individual data of Ca^{2+} response to sufentanil in the presence of vehicle or aticaprant in 15 glomus cells from 6 rats. Data in (B) and (D) represent drug-baseline Ca^{2+}. Horizontal bars in (A) and (C) indicate duration of drug application. ∗∗ and ∗∗∗ denote $P < .01$ and .001, respectively. Wilcoxon signed-rank test in (B), paired *t*-test in (D).

Sham-operated rats showed no change in breathing with vehicle (saline) (Figure 6A, *top panel*). Fentanyl elicited an initial brief stimulation of breathing, followed by respiratory depression (Figure 6A, *middle panel*). The initial stimulation lasted 15–30 s, which was primarily due to increased respiratory rate (Figure 6C–E). The breathing depression lasted 102 ± 14 s. In contrast, CBD rats experienced dramatic breathing depression with apnea, without initial stimulation (Figure 6A, *bottom panel*). In CBD rats, the onset of breathing depression by fentanyl was faster, and the duration was longer compared to sham-operated controls (Figure 6F and G).

IV administration of a KOR agonist (U-50488; 30 μgm/kg, iv) stimulated breathing without respiratory depression (Figure 6B, *top panel*). This breathing stimulation was primarily due to an increased respiratory rate rather than tidal volume (Figure 6B, *top panel*, and 6H and I). In contrast, the KOR agonist did not stimulate breathing in carotid body-denervated rats (Figure 6B, *bottom panel*, Figure 6H and I).

KOR Agonist Reduces Fentanyl-Evoked Respiratory Depression

We then examined whether KOR agonist reduces fentanyl-induced respiratory depression. This possibility was assessed with systemic administration (iv) of fentanyl (30 μgm/kg) combined with KOR agonist (30 μgm/kg). We chose 30 μgm/kg fentanyl, as it is the human equivalent dose used for major surgery and produced severe respiratory depression with apnea in preliminary experiments. Administration of 30 μgm/kg fentanyl alone caused robust respiratory depression with apnea (Figure 7A, *top panel*). Administration of the same dose of fentanyl along

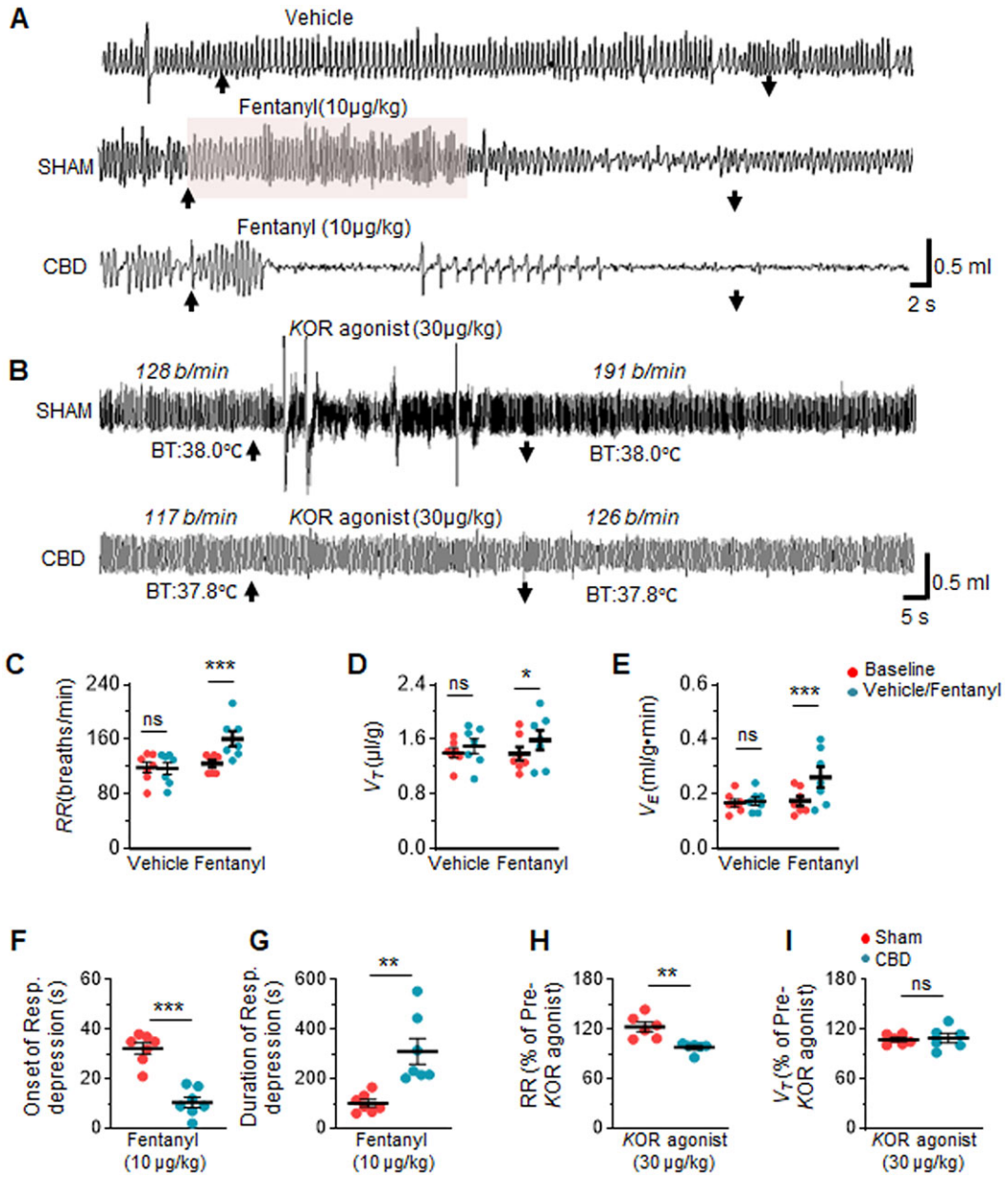

Figure 6. Breathing response to fentanyl and KOR agonist in unanesthetized rats. (A) Examples of breathing responses to iv administration of vehicle (saline, *top panel*) or fentanyl in sham operated (SHAM) (*middle panel*) and CBD (*bottom panel*) rats. (B) Examples of breathing responses to a KOR agonist (U-50488H) in sham operated (SHAM, *top panel*) and carotid body-denervated (CBD, *bottom panel*) rats. Arrows indicate duration of drug application. Shaded area in A represents initial brief stimulation of breathing by fentanyl. b/min in B represents breaths per min and BT body temperature. (C-E) Mean ± SEM and individual data of respiratory rate (RR, C) tidal volume (V_T, D) and minute ventilation (V_E, E) during initial breathing stimulation with iv administration of fentanyl or vehicle in 7 unanesthetized rats. ∗ and ∗∗∗ denote $P < .05$ and $P < .001$, respectively; ns, denotes $P > .05$. Two-way ANOVA with repeated measures followed by the Holm–Sidak test. (F-G) Mean ± SEM and individual data of onset (F) and duration (G) of respiratory depression by fentanyl in sham and CBD rats ($n = 7$ rats each). ∗∗ and ∗∗∗ denote $P < .01$ and .001, respectively. Mann–Whitney rank sum test in F and *t*-test in G. (H-I). Mean ± SEM and individual data of respiratory rate (RR, H) and tidal volume (V_T, I) in response to KOR agonist in sham and CBD rats ($n = 6$ rats each). ∗∗ and ns denote $P < .01$ and $P > .05$, respectively, *t*-test.

with a KOR agonist dramatically reduced fentanyl-induced respiratory depression (Figure 7A, *middle panel*, and Figure 7B). This reduced respiratory depression with KOR agonist was absent in carotid body-denervated rats (Figure 7A, *bottom panel*, and Figure 7B).

Discussion

Present study tested the hypothesis that fentanyl inhibits carotid body afferent nerve activity facilitating respiratory depression (OIRD). Contrary to the hypothesis, fentanyl and its analogue sufentanil stimulated carotid body afferent nerve activity and increased intracellular calcium concentration ($[Ca^{2+}]_i$) in glomus cells via KORs. In unanesthetized rats, fentanyl initially stimulated breathing, followed by respiratory depression. Carotid body-denervated rats experienced only severe respiratory depression (apnea) with fentanyl. A KOR agonist stimulated breathing and, when combined with fentanyl, markedly reduced OIRD, and this effect was absent in carotid body-denervated rats. These findings highlight a previously

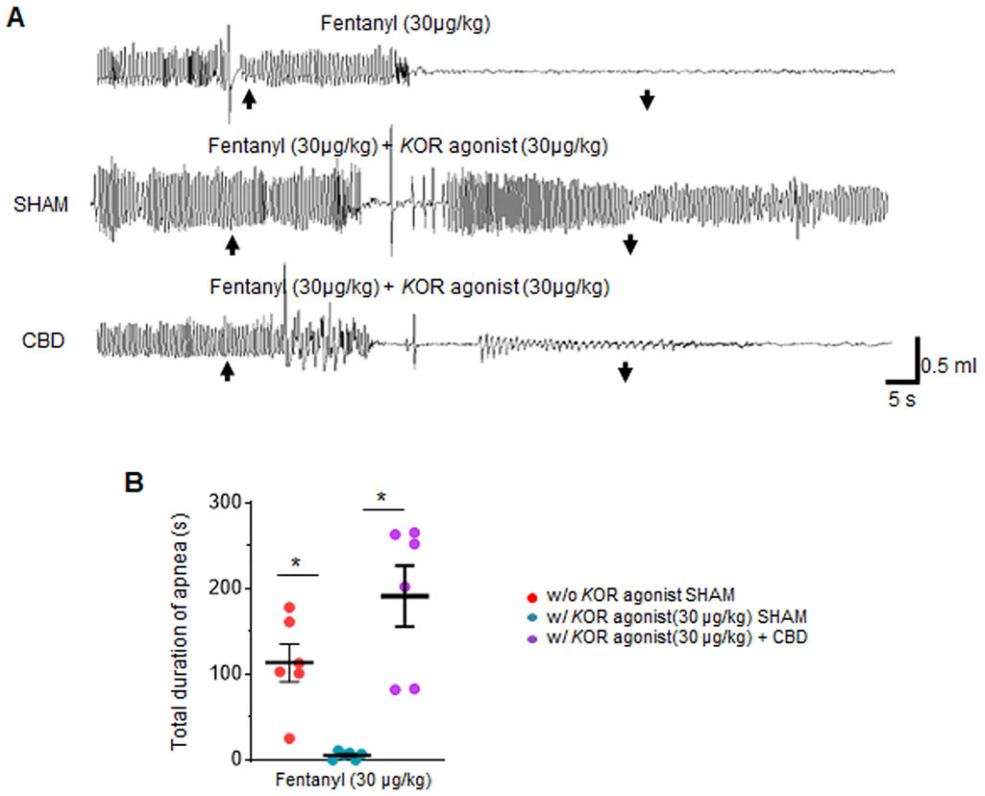

Figure 7. A KOR agonist reduces breathing depression by fentanyl in intact carotid body but not in carotid body-denervated unanesthetized rats. (A) Examples of breathing responses to iv administration of fentanyl alone (*top panel*) and fentanyl + KOR agonist (U-50488H) in sham operated (*middle panel*) and carotid body-denervated (CBD) (*bottom panel*) rats. Arrows indicate duration of drug application. (B) Mean ± SEM and individual data of duration of apnea induced by fentanyl alone or in the presence of KOR agonist in sham and CBD rats ($n = 6$ each). ∗ Indicate $P < .05$. One-way ANOVA on rank followed by Tukey test.

uncharacterized role of KOR in mitigating OIRD through carotid body activation.

Earlier studies[21,22] suggested that opiates inhibit carotid body afferent nerve activity, prompting us to hypothesize that fentanyl also inhibits the carotid body neural activity. Contrary to our hypothesis, fentanyl stimulated the carotid body afferent nerve activity in anesthetized rats, with effects associated with changes in BP (Figure 1). While carotid body activation by fentanyl might be secondary to BP changes, this is unlikely because fentanyl stimulated neural activity in *ex vivo* superfused carotid bodies in a dose-dependent manner, independent of BP. Sufentanil, a fentanyl analogue, also activated the carotid body at nanomolar concentrations, compared to micromolar concentrations of fentanyl, findings consistent with sufentanil being 5–15 times more potent than fentanyl.[36,37] These results demonstrate that fentanyl and sufentanil activate carotid body afferents, similar to activation of pulmonary vagal C fiber afferents by morphine sulfate as reported earlier.[18]

Naloxone blocked carotid body activation by fentanyl, indicating involvement of OR(s). Naloxone binds to μ opioid receptors (MORs) with high affinity, but depending on concentration, it can also block other ORs.[17,38] RNA sequencing and immunohistochemistry showed undetectable levels of μ and δ but a high abundance of κ ORs in glomus cells, as evidenced by co-localization with TH. Although MORs were not evident in the carotid body, MOR-like immunoreactivity was observed in the preBötC consistent with an earlier report.[35] mRNA encoding KORs was reported in DBX-positive preBötC in neonatal mice.[39] We were unable to detect KOR-like immunoreactivity in the preBötC, but it was evident in raphe neurons. This suggests the antibodies used in this study adequately recognize MORs and KORs in rat tissues. The discrepancy between our results and Hayes et al.[39] may be due to age and species variations, as we used adult rats, unlike the neonatal mice used by Hayes et al.[39] or differences in mRNA translation to KOR protein. Furthermore, DAMGO, a selective MOR agonist had no effect, whereas a KOR agonist stimulated carotid body afferent activity similarly to fentanyl, consistent with RNA sequencing and immunohistochemistry data.

Cytosolic $[Ca^{2+}]_i$ elevation in glomus cells is essential for carotid body activation. Fentanyl and sufentanil elevated $[Ca^{2+}]_i$ in glomus cells and aticaprant, a KOR antagonist completely blocked the Ca^{2+} response to both fentanyl and sufentanil, indicating KORs mediate this response. These findings, along with the blockade of carotid body activation by KOR antagonist, demonstrate that KORs are the primary ORs mediating carotid body activation by fentanyl and its analogue sufentanil. ORs are G protein-coupled receptors, generally coupled to Gi or Go proteins, and inhibit $[Ca^{2+}]_i$ elevation.[40] However, κ-OR activation was reported to increase $[Ca^{2+}]i$ by interacting with $G\alpha q$ in cell lines.[41,42] Further studies are needed to establish the mechanism(s) underlying Ca^{2+} elevation by fentanyl and sufentanil.

Fentanyl initially stimulates breathing albeit briefly, followed by respiratory depression. In contrast, carotid body-denervated rats show only severe respiratory depression with apnea without initial breathing stimulation. These findings are reminiscent of breathing stimulation by morphine.[43] The following observations demonstrate that the initial respiratory stimulation is mediated by the carotid body: (1) CBD rats exhibit absence of breathing stimulation by fentanyl and (2) fentanyl stimulate

carotid body afferent nerve activity. Given that fentanyl crosses the blood-brain barrier, respiratory depression is likely due to its central depressive action on brainstem neurons. Fentanyl-induced respiratory depression causes hypoxemia and elevate arterial CO_2 levels, which are "physiological" activators of the carotid body afferents. The effects of fentanyl and/or sufentanil on the carotid body response to hypoxia and CO_2 remain to be investigated. Nonetheless, the severe respiratory depression with apnea observed in carotid body-denervated rats, compared to the modest inhibition of breathing with intact carotid bodies, suggests that fentanyl's activation of carotid body afferents may counteract its central inhibitory action.

A KOR agonist stimulated breathing in unanesthetized rats but did not depress breathing like fentanyl. Carotid body mediates breathing stimulation by KOR agonist, as indicated by (1) KOR agonist activated carotid body afferents and (2) breathing stimulation by KOR agonist is absent in CBD rats. KOR agonist also stimulates breathing in turtles.[44] However, unlike rats, KOR agonist stimulates breathing in turtles primarily by increasing tidal volume.

An intriguing finding of this study is that a KOR agonist nearly blocked respiratory depression by fentanyl in unanesthetized rats. This effect is due to the activation of the carotid body, as indicated by (a) the absence of protective effects KOR agonist on fentanyl-induced breathing depression in carotid body-denervated rats, and (b) activation of carotid body afferent nerve activity by KOR agonist. Although KOR agonists may affect body temperature,[45,46] this effect is unlikely to accounts in the present study because body temperature remained unchanged with KOR agonist in unanesthetized rats (Figure 6B). These findings suggest that activating the carotid body with a KOR agonist might offer a therapeutic intervention for mitigating OIRD without compromising analgesic properties of fentanyl, as KOR agonists do not affect analgesia.[47] While these indicate potential therapeutic application of KOR agonist in mitigating OIRD with fentanyl doses used clinically, it remains to be established whether KOR agonists can block OIRD with higher doses of fentanyl.

Authors Contributions

Ying-Jie Peng (Data curation, Formal analysis, Investigation, Methodology, Validation, Visualization), Jayasri Nanduri (Data curation, Formal analysis, Investigation, Methodology, Supervision, Validation), Ning Wang (Data curation, Formal analysis, Investigation, Methodology, Validation, Visualization), Zheng Xie (Resources), Aaron P. Fox (Resources), Nanduri R. Prabhakar (Conceptualization, Funding acquisition, Project administration, Supervision, Validation, Writing – original draft, Writing – review & editing).

Supplementary Material

Supplementary material is available at the *APS Function* online.

Funding

This work is supported by the National Institutes of Health (NIH) grant HL-174373.

Conflict of Interest

None declared.

Data Availability

All data and materials used in the analysis are available in some form to any researcher for purposes of reproducing or extending the analysis.

References

1. Denavit-Saubié M, Champagnat J, Zieglgänsberger W. Effects of opiates and methionine-enkephalin on pontine and bulbar respiratory neurones of the cat. *Brain Res* 1978;**155**(1):55–67.
2. Brackley AD, Andrade MA, Toney GM. Intermittent hypercapnic hypoxia induces respiratory hypersensitivity to fentanyl accompanied by tonic respiratory depression by endogenous opioids. *J Physiol* 2020;**598**(15):3239–3257.
3. Ren J, Ding X, Funk GD, Greer JJ. Ampakine CX717 protects against fentanyl-induced respiratory depression and lethal apnea in rats. *Anesthesiology* 2009;**110**(6):1364–1370.
4. Saunders SE, Levitt ES. Kölliker–Fuse/Parabrachial complex mu opioid receptors contribute to fentanyl-induced apnea and respiratory rate depression. *Respir Physiol Neurobiol* 2020;**275**:103388.
5. Seckler JM, Grossfield A, May WJ, Getsy PM, Lewis SJ. Nitrosyl factors play a vital role in the ventilatory depressant effects of fentanyl in unanesthetized rats. *Biomed Pharmacother* 2022;**146**:112571.
6. Varga AG, Reid BT, Kieffer BL, Levitt ES. Differential impact of two critical respiratory centres in opioid-induced respiratory depression in awake mice. *J Physiol* 2020;**598**(1):189–205.
7. Vasilakos K, Wilson RJ, Kimura N, Remmers JE. Ancient gill and lung oscillators may generate the respiratory rhythm of frogs and rats. *J. Neurobiol.* 2005;**62**(3):369–385.
8. Johnson SM, Moris CM, Bartman ME, Wiegel LM. Excitatory and inhibitory effects of opioid agonists on respiratory motor output produced by isolated brainstems from adult turtles (Trachemys). *Respir Physiol Neurobiol* 2010;**170**(1):5–15.
9. Kharbush RJ, Gutwillig A, Hartzler KE, et al. Antinociceptive and respiratory effects following application of transdermal fentanyl patches and assessment of brain μ-opioid receptor mRNA expression in ball pythons. *Am J Vet Res* 2017;**78**(7):785–795.
10. Mutolo D, Bongianni F, Einum J, Dubuc R, Pantaleo T. Opioid-induced depression in the lamprey respiratory network. *Neuroscience* 2007;**150**(3):720–729.
11. Ramirez JM, Burgraff NJ, Wei AD, et al. Neuronal mechanisms underlying opioid-induced respiratory depression: our current understanding. *J Neurophysiol* 2021;**125**(5):1899–1919.
12. Lalley PM. Mu-opioid receptor agonist effects on medullary respiratory neurons in the cat: evidence for involvement in certain types of ventilatory disturbances. *Am J Physiol-Regul Integr Comp Physiol* 2003;**285**(6):R1287–R1304.
13. Levitt ES, Abdala AP, Paton JF, Bissonnette JM, Williams JT. μ opioid receptor activation hyperpolarizes respiratory-controlling Kölliker–Fuse neurons and suppresses post-inspiratory drive. *J Physiol* 2015;**593**(19):4453–4469.
14. Montandon G, Horner R. CrossTalk proposal: the pre-Botzinger complex is essential for the respiratory depression following systemic administration of opioid analgesics. *J Physiol* 2014;**592**(6):1159–1162.
15. Prkic I, Mustapic S, Radocaj T, et al. Pontine μ-opioid receptors mediate bradypnea caused by intravenous remifentanil

infusions at clinically relevant concentrations in dogs. *J Neurophysiol* 2012;**108**(9):2430–2441.
16. Saunders SE, Baekey DM, Levitt ES. Fentanyl effects on respiratory neuron activity in the dorsolateral pons. *J Neurophysiol* 2022;**128**(5):1117–1132.
17. Dhawan BN, Cesselin F, Raghubir R, et al. International Union of Pharmacology. XII. Classification of opioid receptors. *Pharmacol Rev* 1996;**48**(4):567–592.
18. Willette RN, Sapru HN. Peripheral versus central cardiorespiratory effects of morphine. *Neuropharmacology* 1982;**21**(10):1019–1026.
19. Zhuang J, Gao X, Shi S, Xu F. Intravenous bolus injection of fentanyl triggers an immediate central and upper airway obstructive apnea via activating vagal sensory afferents. *J Appl Physiol* 2024;**137**(6):1666–1677.
20. Kumar P, Prabhakar NR. Peripheral chemoreceptors: function and plasticity of the carotid body. *Com Physiol* 2012;**2**(1):141–219.
21. McQueen DS, Ribeiro JA. Inhibitory actions of methionine-enkephalin and morphine on the cat carotid chemoreceptors. *British J Pharmacology* 1980;**71**(1):297–305.
22. Pokorski M, Lahiri S. Effects of naloxone on carotid body chemoreception and ventilation in the cat. *J Appl Physiol Respir Environ Exerc Physiol* 1981;**51**(6):1533–1538.
23. Peng YJ, Prabhakar NR. Measurement of sensory nerve activity from the carotid body. *Methods Mol Biol* 2018;**1742**:115–124.
24. Peng YJ, Gridina A, Wang B, Nanduri J, Fox AP, Prabhakar NR. Olfactory receptor 78 participates in carotid body response to a wide range of low O_2 levels but not severe hypoxia. *J Neurophysiol* 2020;**123**(5):1886–1895.
25. Yuan G, Peng YJ, Khan SA, et al. H2S production by reactive oxygen species in the carotid body triggers hypertension in a rodent model of sleep apnea. *Sci Signal* 2016;**9**(441):ra80.
26. Peng YJ, Nanduri J, Wang N, et al. Hypoxia sensing requires H2S-dependent persulfidation of olfactory receptor 78. *Sci Adv* 2023;**9**(27):eadf3026.
27. Wang N, Peng YJ, Kang W, Hildreth M, Prabhakar NR, Nanduri J. Transcriptomic analysis of postnatal rat carotid body development. *Genes* 2024;**15**(3):302.
28. Browe BM, Peng YJ, Nanduri J, Prabhakar NR, Garcia AJ, 3rd. Gasotransmitter modulation of hypoglossal motoneuron activity. *eLife* 2023;**12**:e81978.
29. Paxinos G, Watson C. *The Rat Brain in Stereotaxic Coordinates*. Burlington, MA, USA: Academic Press, 2006.
30. Nanduri J, Peng YJ, Wang N, et al. Epigenetic regulation of redox state mediates persistent cardiorespiratory abnormalities after long-term intermittent hypoxia. *J Physiol* 2017;**595**(1):63–77.
31. Peng YJ, Zhang X, Gridina A, et al. Complementary roles of gasotransmitters CO and H2S in sleep apnea. *Proc Natl Acad Sci USA* 2017;**114**(6):1413–1418.
32. Hospira. *Fentanyl Citrate Injection, USP [Labeling-Package Insert]*. U.S. Food and Drug Administration. https://www.accessdata.fda.gov/drugsatfda_docs/label/2023/019115s042lbl.pdf . Accessed 20 December 2023.
33. Nanduri J, Prabhakar NR. Immunohistochemistry of the Carotid Body. *Methods Mol Biol* 2018;**1742**:155–166.
34. Gray PA, Janczewski WA, Mellen N, McCrimmon DR, Feldman JL. Normal breathing requires pre-Bötzinger complex neurokinin-1 receptor-expressing neurons. *Nat Neurosci* 2001;**4**(9):927–930.
35. Gray PA, Rekling JC, Bocchiaro CM, Feldman JL. Modulation of respiratory frequency by peptidergic input to rhythmogenic neurons in the pre-Botzinger complex. *Science* 1999;**286**(5444):1566–1568.
36. Monk JP, Beresford R, Ward A. Sufentanil. A review of its pharmacological properties and therapeutic use. *Drugs* 1988;**36**(3):286–313.
37. Oh SK, Lee IO, Lim BG, et al. Comparison of the analgesic effect of sufentanil versus fentanyl in intravenous patient-controlled analgesia after total laparoscopic hysterectomy: a randomized, double-blind, prospective study. *Int J Med Sci* 2019;**16**(11):1439–1446.
38. Ritter J, Flower RJ, Henderson G, et al. *Rang and Dale's Pharmacology*. London: Elsevier, 2024.
39. Hayes JA, Kottick A, Picardo MCD, et al. Transcriptome of neonatal pre-Bötzinger complex neurones in Dbx1 reporter mice. *Sci Rep* 2017;**7**(1):8669.
40. Hille B. Modulation of ion-channel function by G-protein-coupled receptors. *Trends Neurosci* 1994;**17**(12):531–536.
41. Jin W, Lee NM, Loh HH, Thayer SA. Dual excitatory and inhibitory effects of opioids on intracellular calcium in neuroblastoma x glioma hybrid NG108-15 cells. *Mol Pharmacol* 1992;**42**(6):1083–1089.
42. Spencer RJ, Jin W, Thayer SA, Chakrabarti S, Law PY, Loh HH. Mobilization of Ca2+ from intracellular stores in transfected neuro2a cells by activation of multiple opioid receptor subtypes. *Biochem Pharmacol* 1997;**54**(7):809–818.
43. Baby SM, Gruber RB, Young AP, MacFarlane PM, Teppema LJ, Lewis SJ. Bilateral carotid sinus nerve transection exacerbates morphine-induced respiratory depression. *Eur J Pharmacol* 2018;**834**:17–29.
44. Johnson SM, Kinney ME, Wiegel LM. Inhibitory and excitatory effects of micro-, delta-, and kappa-opioid receptor activation on breathing in awake turtles, *Trachemys scripta*. *Am J Physiol-Regul Integr Comp Physiol* 2008;**295**(5):R1599–R1612.
45. Adler MW, Geller EB, Rosow CE, Cochin J. The opioid system and temperature regulation. *Annu Rev Pharmacol Toxicol* 1988;**28**(1):429–449.
46. Xin L, Geller EB, Adler MW. Body temperature and analgesic effects of selective mu and kappa opioid receptor agonists microdialyzed into rat brain. *J Pharmacol Exp Ther* 1997;**281**(1):499–507.
47. Dalefield ML, Scouller B, Bibi R, Kivell BM. The kappa opioid receptor: a promising therapeutic target for multiple pathologies. *Front Pharmacol* 2022;**13**:837671.

Submitted: 5 February 2025; **Revised:** 1 May 2025; **Accepted:** 10 May 2025